JAAS

Cite this: *J. Anal. At. Spectrom.*, 2012, **27**, 1110

www.rsc.org/jaas

PAPER

Laser-induced breakdown spectroscopy for analysis of micro and nanoparticles

Prasoon K. Diwakar,[a] Kristofer H. Loper,[c] Anna-Maria Matiaske[b] and David. W. Hahn*[c]

Received 17th January 2012, Accepted 18th April 2012
DOI: 10.1039/c2ja30012e

The use of laser-induced breakdown spectroscopy (LIBS) for analysis of micro- and nanoparticles is explored, including a brief review of the recent research, both fundamentals and applications, along with new experimental work regarding aerosol particle sampling statistics, analysis of laser ablation particles *via* aerosol LIBS for matrix effect minimization for bulk solids analysis, and a novel aerosol particle concentration scheme that is suited for near real-time analysis of aerosol nanoparticles. The statistical analysis reveals that the LIBS particle sampling physics are well modeled using Poisson sampling statistics, as based on analysis of calcium-rich ambient air particles. The laser-ablation LIBS (LA-LIBS) methodology was explored for a range of disparate metallic and non-metallic bulk samples, revealing a linear calibration curve for all six samples over the range of relative Mn/Fe mass concentrations. Finally, the microneedle concentration technique for aerosol nanoparticle analysis was successfully demonstrated with linear mass calibration curves for copper-rich nanoparticles. Overall, a fundamental understanding of the plasma–particle physics has enabled the formulation of robust LIBS-based nanoparticle schemes.

Background and review

Laser-induced Breakdown Spectroscopy (LIBS) has attained significant success and popularity for analysis of a variety of materials including solids, liquids, gases and aerosols. LIBS has found applications in a variety of fields, although here the attention is on aerosol particle analysis, notably ultrafine particles, including particles generated *via* laser ablation. Research studies related to both applications as well as fundamental understanding of the relevant LIBS processes have been pursued by several research groups, which has helped the success of LIBS as an analytical approach, although unique challenges remain in performing nanoparticle analysis. Difficulties in analyzing nanoparticles using LIBS lie in the nature of the LIBS plasma (*e.g.* highly transient, non-homogeneous, and non-LTE), as well as the consequent complexities involved in plasma–particle interactions. The complex nature of such interactions results in issues such as particle sampling, matrix and fractionation effects, locally non-equilibrium conditions, and incomplete vaporization, which together pose serious challenges for quantitative analysis. Nevertheless, recent studies on analysis of particles using LIBS have shed light on the fundamental aspects, as well as many potential applications. In the following brief review of the recent literature, we present here a summary of relevant issues pursuant to nanoparticle analysis, followed by our recent experimental results covering particle sampling and two novel LIBS schemes.

Hahn and co-workers addressed in their early work many of the aspects related to the discrete nature of plasma–particle interactions for direct LIBS analysis of aerosol systems.[1–3] Important topics reported include the finite laser-induced plasma volume (~1 mm^3) in the context of the particle sampling methodology and statistical averaging of LIBS spectral data. As elaborated on below with the first set of experimental data, it is important to appreciate the role of statistics for particle analysis *via* LIBS, in that the statistical distribution of the resulting analytical signal defines the ability for single particle measurements. Following the progression from particle sampling, it is necessary to understand the interactions between the individual particles and the laser-induced plasma. As first demonstrated by Hohreiter *et al.* using direct imaging of plasma–particle interactions within a laser-induced plasma, the particle-derived analyte species are initially confined to discrete regions of the plasma, diffusing at a finite rate through the plasma *via* mass transfer.[4] As summarized recently,[5] quantitative analysis of aerosol particles by LIBS requires a thorough understanding of the relevant physical processes, namely heat and mass transfer, which govern the dissociation, vaporization, ionization and ultimately the atomic excitation, of analyte species. These same processes play key roles in particle-related matrix effects, affecting quantitative analysis, and must be carefully understood and mitigated.[6,7]

[a]*National Institute of Occupational Safety and Health, Cincinnati, OH 45213, USA*
[b]*BAM Federal Institute of Materials Research and Testing, Berlin, Germany*
[c]*Mechanical and Aerospace Engineering, University of Florida, Gainesville, FL 32611, USA. E-mail: dwhahn@ufl.edu*

A number of studies have reported applications of LIBS for real-time or near real-time analysis of a wide range of micro- and nanoparticles. Early studies explored the use of LIBS for analysis of lead aerosol particles, including polydisperse particles in the range of 10 to 300 nm, with detection limits in the range of 150 μg m^{-3} using ensemble-averaging,[8] and for aerosol particles in ambient air using real-time conditional analysis for single-particle detection at overall magnesium concentrations of a few parts per trillion (mass) and absolute particle mass in the range of a few femtograms.[9] The investigation of LIBS specifically for on-line monitoring of nanoparticles was reported by Amodeo *et al.*,[10] successfully demonstrating quantitative analysis of silicon carbide nanoparticles in the size range of 20 to 100 nm. Noll *et al.* reported size-resolved (20 to 800 nm) measurements of ultrafine particulate matter using LIBS for analysis of $CaCl_2$ particles.[11] They reported calibration curves showing a correlation between analyte signal and mass concentration; however, non-linearities were observed for the larger particle sizes. In another study, LIBS-based aerosol analysis for monitoring of air pollution was investigated, including direct *in situ* analysis and an indirect approach using filter enrichment.[12] Direct analysis revealed a linear particle mass-based response for copper-rich particles up to a diameter of about 7 μm, and linear calibration curves within the corresponding regime of total particle vaporization. The indirect analysis (*i.e.* filter collection) was found to be more efficient with regard to sample particle numbers, but better detection limits were found with the direct analysis. A recent LIBS-based scheme for aerosol analysis uses a novel particle collection scheme to pre-concentrate aerosol particles on the tip of a fine needle, where they subsequently undergo direct analysis by the laser-induced plasma.[13] This approach yields pg to ng sensitivity, and avoids the problem of ultralow particle sampling rates with direct *in situ* LIBS nanoparticle analysis under dilute concentrations. Another recent study examined LIBS for direct analysis of carbon nanotubes (CNTs) in combination with TEM analysis of sampled particles, in which the coupled approach was seen as promising for real-time detection of CNTs.[14]

Laser-induced breakdown spectroscopy has been used in other methodologies to achieve analysis of micro-particles and micro-droplets. Several papers have explored the use of LIBS for ultralow sample volume droplets (*e.g.* sub-nanolitre), including in conjunction with liquid chromatography,[15] and directly in aerosol form using a monodisperse microdroplet generator.[16] Groh *et al.* were able to achieve low sample introduction volumes in sub-nanolitre to picolitre range, and excellent absolute detection limits for gold and calcium were obtained.[16] Overall, both schemes offer nearly 100% efficient droplet sampling; hence are well-suited for analysis of limited analyte volumes. Analyzing single micro-droplets and particles in analytical plasmas can additionally provide great insight into various fundamental processes, namely vaporization, desolvation, atomization, plasma–particle interaction, and so on. For example, Diwakar *et al.* were able to estimate the mass diffusion coefficient of atomic hydrogen by using micro-droplets combined with imaging experiments.[7] Laserna *et al.* report a scheme referred to as optical catapulting designed for LIBS analysis of aerosol particles ejected from a deposited substrate using a laser pulse as the driving force.[17] The technique was successfully demonstrated for aluminium silicate, nickel, quartz and stainless steel particles. Windom and Hahn used aerosol LIBS analysis following laser-ablation as a means to mitigate matrix effects typically associated with direct LIBS analysis of solids.[18] By transporting the laser ablation plume of fine particles to an air-breakdown LIBS plasma, which serves as the analytical plasma analogous to the inductively coupled plasma in LA-ICP-OES, considerable improvements in relative analyte response were achieved for a range of metallic samples, as compared to direct LIBS analysis of the same solids, demonstrating a mitigation of bulk matrix effects. Such an approach allows one to take advantage of the understanding of plasma–particle interactions associated with aerosol LIBS to maximize the aerosol analyte response and mitigate potential matrix effects, while avoiding the many complexities involved in direct laser-bulk sample interactions. Working toward smaller sample volumes and lower limits for absolute mass analysis, LIBS offers the opportunity for single-shot analysis, as reported in a recent review paper.[19] Taken to the limit, LIBS has the ability for analysis of extremely small absolute mass quantities, with masses as low as 220 ag reported recently for femtosecond LIBS.[20] Such low limits have not been reported to date for direct analysis of aerosol nanoparticles, although single-particle masses at the single fg level have been reported with aerosol LIBS.[21] Clearly LIBS is applicable for analysis of micro- and nanoparticles under a wide range of applications and experimental configurations.

We now present some recent experimental results concerning the sampling statistics associated with direct LIBS-based analysis of aerosol systems, followed by laser-ablation LIBS (LA-LIBS) data for a disparate range of sample matrices (including metallic and non-metallic samples), and finally, results of a novel aerosol nanoparticle concentration scheme that is well-suited for real-time monitoring under low aerosol loadings and/or analyte mass concentrations.

Sampling issues: conditional analysis and Poisson statistics

Sampling of aerosol particles with the LIBS technique differs from sampling in other analytical techniques. In many analytical techniques, the analyte sample is introduced as a continuous stream into the analytical plasma and the resulting signal is integrated in time, which provides measurement of the average analyte concentration in the plasma volume, often maximizing the signal-to-noise ratio. Consider for example, inductively coupled plasma mass spectrometry (ICP-MS), where the plasma forms a steady-state source of vaporization, and the analyte is introduced into the plasma volume at a continuous rate *via* nebulization. Comparing ICP-MS, or even direct LIBS analysis of bulk solids, to aerosol sampling with LIBS, reveals a different and more complex scenario. Because the LIBS plasma volume is finite in nature, coupled with the discrete nature of the aerosol particles, a complex sampling problem emerges and may call for a different approach for signal analysis than the traditional ensemble-averaging methods generally used with LIBS. For aerosols, such a sampling and analysis method may potentially offer no response or an extremely weak analyte response for the presence of a dilute analyte in the sample. In order to increase the response for LIBS analysis, a sequence of spectral signals (*i.e.*

single spectra) is recorded, with each LIBS plasma volume considered a unique sampling event. Then each individual LIBS spectrum may be examined for the presence of the targeted analyte emission lines, corresponding to the presence of a single analyte particle or particles, and by optimal gating, signal collection, and processing schemes, aerosol systems can be effectively studied using LIBS.

Such a conditional analysis of aerosols provides the opportunity to discard signals which have no analyte response, while considering only those spectra for analysis which have an analyte response beyond a threshold limit. This technique has been developed and discussed in detail in earlier works of Hahn and co-workers.[1,2] Discreteness of the analyte-containing particles with respect to the plasma volume is key when considering LIBS for conditional aerosol analysis. Ambient air, a natural system with dilute aerosol particles, serves as an opportune aerosol source for understanding the sampling process and sampling statistics, and was therefore used in this study. In particular, discrete aerosol sampling statistics in the context of LIBS are conveniently modeled using Poisson statistics,[2] where we define

$$P_n = \frac{\mu^n}{n!} e^{-\mu} \quad (1)$$

where P_n is the probability of sampling n number of discrete aerosol particles in a given plasma volume, noting that n is an integer, and where μ is the average number of particles per plasma volume, namely,

$$\mu = N\, V_{\text{plasma}} \quad (2)$$

readily calculated as the product of the particle number density (particles per unit volume of gas) and the effective plasma sampling volume.[22]

The modeling of aerosol sampling in LIBS plasmas using Poisson statistics enables a theoretical contribution of aerosol particles as discrete analyte masses, thereby enabling one to look into key sampling regimes and to identify appropriate algorithms such as ensemble-averaging or conditional analysis, or perhaps particle pre-concentration approaches. As revealed in earlier studies, sampling rates well below 1% are commonly encountered when studying ambient air.[23] For such cases it is important that LIBS aerosol analysis be analyzed and modeled accordingly, taking into consideration discrete particles and discrete plasma volume. For example, it has been shown that a minimum of 20 shots provides a reasonable representation of a typical aerosol sample, using Monte Carlo simulations in combination with a Poisson distribution.[1] Such statistical considerations are important in LIBS particle sampling, although to date no systematic measurements have directly assessed the applicability of the Poisson distribution. Such an analysis is one goal of the present work.

As discussed above, aerosol sampling in LIBS may be modeled using the Poisson distribution, which is defined as a discrete probability distribution used for modeling of random samples or events which are rare and independent from each other.[24] The number of expected events, in our case the number of discrete aerosol particles sampled by a given laser-induced plasma volume was given above by eqn (1), where μ is a positive real number. We also note that μ gives the variance of the distribution, which implies that the mean number of occurrences fluctuate about the mean value μ by standard deviation $\sqrt{\mu}$, which are also referred to as Poisson noise. The value of single occurrences sometimes might be too small to measure, and in such cases correlation of Poisson noise with the mean value gives a measure of the contribution of single occurrences to the whole process.

The current experimental setup is identical to the configuration reported previously.[23] The LIBS setup consists of a Q-switched Nd:YAG laser operating at the fundamental wavelength of 1064 nm (5 Hz repetition rate), 10 ns pulse width, laser energy of 290 mJ per pulse, which was focused to create the laser-induced plasma using a 50 mm diameter, 75 mm focal length UV-grade lens at the center of six-way cross LIBS chamber. The LIBS signal was collected on the axis of the incident beam in backscatter using a pierced mirror and 75 mm condensing lens, and then focused to a fiber optic bundle and coupled to a 0.275 m spectrometer (2400 groove mm^{-1} grating, 0.15 nm resolution). Backscatter collection of the plasma emission ensured minimal spatial variation in the LIBS signal. Finally the plasma emission was recorded on an ICCD detector array, which was synchronized to the laser Q-switch, and further connected to the computer for analysis.

Ambient air was drawn into the chamber through a US EPA PM 2.5 sampling inlet (Rupprecht and Patashnick), which only passes particulate sizes of 2.5 microns or less. This particular sampling inlet and location has been described in detail by Hettinger *et al.*[23] The inlet, with a constant sampling rate of 1 m^3 h^{-1}, was located 5 m above the ground adjacent to a three story building. The transfer line brought the sampled air from inlet to the LIBS chamber, ensuring minimal transport losses. The outlet of the six-way cross chamber was connected to vacuum pump which provided the bulk sampling flow rate from the inlet to the LIBS chamber, with pressure in the chamber maintained at about 0.74 torr below atmospheric pressure.

Ionic calcium emission lines at 393.37 nm (0–24,414 cm^{-1}) and 396.85 nm (0–29,192 cm^{-1}) were chosen to analyze ambient air particulate data with a fixed detector delay of 40 μs and integration time of 40 μs. This provided the optimal signal-to-noise ratio for Ca lines owing to decay of continuum emission, as determined through experimentation. Calcium was targeted as a common analyte species in ambient air dust particulates, as calcium is a common crustal element. Ambient air was sampled over a period of several days, typically using three sessions during the day (roughly morning, noon and evening). The three different sessions were chosen to provide as wide a range of particle concentrations as possible, as the early morning dew point is expected to decrease the concentration due to nucleation and condensation on dust particles and subsequent settling. During each LIBS session, 20 sequences of spectral data were collected consecutively, with each sequence comprised of 1000 laser shots recorded at a frequency of 5 Hz; hence each of the 20 sequences lasted for 3 : 20 min. The total experimental time for each session was just over an hour, and corresponded to 20 000 total laser shots (20 × 1000).

Real-time conditional analysis was used to reject the spectra with no significant signal from the analyte, namely, from the calcium emission lines. To minimize the probability of false hits, a threshold was determined for the signal without any analyte

present (*i.e.* in purified air), specifically, by setting the threshold to about 100% above the observed calcium line peak/base ratio in the absence of any analyte. This algorithm helped to ensure that only true hits were recorded while minimizing the loss of data, as summarized by Carranza and co-workers.[25] The spectra which correspond to real hits were identified using the presence of both Ca peaks for final confirmation, and the sampling statistics were recorded for each 1000-shot sequence.

As noted above, calcium lines at 393.37 nm and 396.85 nm were chosen to analyze the spectral data, providing excellent analyte sensitivity. For example, work with aerosolized spores in the same system revealed a calcium absolute detection limit of about 2 femtograms.[21] Such a detection limit corresponds to a single dust particle of about 200 nm, where the Ca containing dust particle has been modeled as calcium carbonate, $CaCO_3$, a common mineral in ambient air. Fig. 1 shows raw spectral data obtained by ensemble-averaging all 20 000 shots from a 1 hour sequence, along with the ensemble-average of 37 spectra identified to correspond to the sampling of individual aerosol dust particles based on the detection of calcium atomic emission above the detection threshold. The number density can be estimated by considering the plasma volume (1.2 mm^3 as per ref. 22), and the LIBS-based sampling rate given by the ratio of the real hits and the number of laser shots (37/20 000), which gives an average number density of 1.54 particles cm^{-3}. It clearly shows that conditional analysis algorithm increases the signal-to-noise ratio for particle analysis. The additional spectral features in Fig. 1 are attributed to the N_2^+ first positive system (388.4 and 391.4 nm) and to the CN violet system (387.1 and 388.3 nm).

The data present an interesting opportunity to examine the applicability of the Poisson distribution. For each session, LIBS data was collected in 1000-pulse laser sequences, for a total of 20 000 laser pulses (*i.e.* 20 sets of 1000 shots each, as described above). The particular dataset discussed here corresponds to 37 individual particles (Set 1 in Table 1), and as noted above, and to 1541 calcium-rich particles per litre of air. The Poisson parameter is readily calculated as $\mu = 0.00185$, which is the product of the number density and the plasma sample volume. This value of μ may then be multiplied by the number of laser pulses per sampling interval, namely 1000, to yield the expected value of 1.85 particle hits per 1000 pulses. This value of $\mu = 1.85$ may then be used to predict the sampling distribution of calcium-based particle hits per 1000 pulses (*via* eqn (1)), and then directly compared with the measured sampling results from the twenty 1000-shot sequences. The experimental and theoretical values for four different sets of data are tabulated in Table 1.

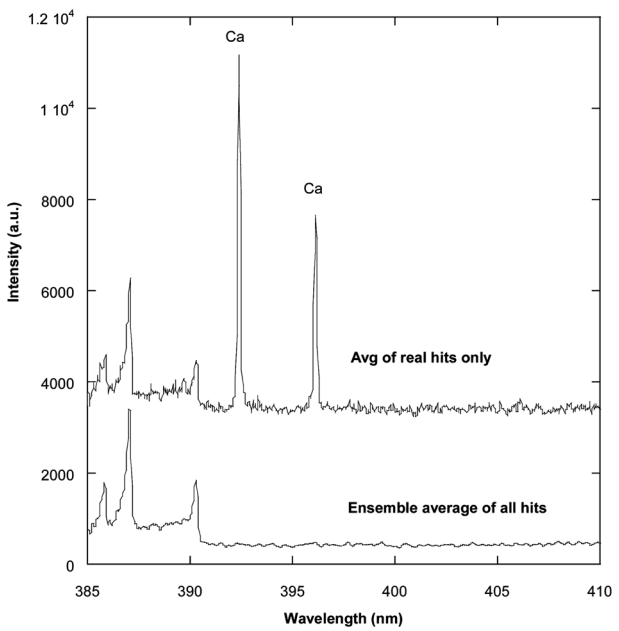

Fig. 1 LIBS spectra recorded in ambient air for the ensemble-average of 20 000 laser shots, and for the subset of 37 spectra corresponding to sampled ambient aerosol dust particles, as based on calcium detection.

The calculated and measured sampling distributions for the four datasets are plotted in Fig. 2 over the representative twenty 1000-pulse data collection intervals. The ideal Poisson distribution and the experimental sampling rates are in very good agreement for all the sets of data. Specifically for set 1, the probability of recording zero particle hits is equal to 15% and 10% for the experimental data and Poisson distribution fits, respectively, while the most probable sampling rate of 2 particles per sequence corresponds to 29.1% and 35% for the predicted and experimental data, respectively. Similar results were found for the other 1 hour datasets with both higher and lower average sampling rates. Overall, the plots demonstrate the statistical nature of LIBS-based aerosol sampling, and provides corroboration of Poisson-based model to describe the LIBS sampling problem.

Mitigation of matrix effects using LA-LIBS

As noted above, the unique combination of laser-ablation and LIBS-based aerosol analysis provides an opportunity to independently optimize both the laser-ablation (*i.e.* material sampling) and the plasma–particle interactions (*i.e.* analyte measurement) through a concept referred to as LA-LIBS, as previously reported.[18] Direct analysis of bulk materials with LIBS provides a range of complexities due to the use of the same laser pulse and subsequent laser-induced plasma for all physical processes, including vaporization, dissociation, and atomic excitation. However, LA-LIBS separates the analyte sampling from the quantitative analyte measurement, allowing the latter process to be fully optimized using the wide range of knowledge gained as to the physics of aerosol nanoparticle analysis. Here we demonstrate the LA-LIBS approach for a disparate set of solid samples, including both metallic and non-metallic bulk samples.

The experimental set-up is similar to that reported previously by Windom and Hahn,[18] although several modifications were made with a goal of improving the ablation process and the subsequent transport of the ablation plume to the analytical LIBS plasma. Briefly, an ablation chamber was constructed using a 3.5 cm diameter stainless-steel vacuum chamber. The sample target was mounted on a rotating stage (0.25 rev s^{-1}) opposite a UV-grade quartz window.

An approximately 3.2 mm inside diameter tube allowed the nitrogen carrier gas to enter and exit the sample chamber on opposite sides, transporting the ablation particles directly to the free-standing laser-induced plasma in the adjacent sample chamber, as shown in Fig. 3. A 6.5 cm length of tubing was used

Table 1 Experimental and Poisson calcium-containing particle sampling probabilities for each of twenty consecutive 1000-shot sequences recorded in ambient air (4 datasets)

	Set 1				Set 2			
Hits/1000	Events	Total hits	Exp. prob.	Poisson prob.	Events	Total hits	Exp. prob.	Poisson prob.
0	2	0	10	15.72	2	0	10	8.63
1	7	7	35	29.09	3	3	15	21.14
2	5	10	25	26.91	6	12	30	25.90
3	4	12	20	16.59	5	15	25	21.15
4	2	8	10	7.67	3	12	15	12.95
5	0	0	0	2.84	1	5	5	6.35
6	0	0	0	0.88	0	0	0	2.59
7	0	0	0	0.231	0	0	0	0.907
8	0	0	0	0.054	0	0	0	0.278
Total	**20**	**37**	**100**	**99.99**	**20**	**47**	**100**	**99.90**
	Set 3				Set 4			
Hits/1000	Events	Total hits	Exp. prob.	Poisson prob.	Events	Total hits	Exp. prob.	Poisson prob.
0	5	0	25	27.25	1	0	5	3.17
1	6	6	30	35.43	1	1	5	10.95
2	7	14	35	23.03	4	8	20	18.89
3	2	6	10	9.98	6	18	30	21.73
4	0	0	0	3.24	4	16	20	18.74
5	0	0	0	0.84	1	5	5	12.93
6	0	0	0	0.18	1	6	5	7.43
7	0	0	0	0.033	1	7	5	3.66
8	0	0	0	0.005	1	8	5	1.58
Total	**20**	**26**	**100**	**99.99**	**20**	**69**	**100**	**99.09**

connect the ablation chamber to the analytical LIBS chamber, thereby minimizing any sample losses during transport. A vacuum pump was used to draw nitrogen gas through the ablation chamber and the LIBS sample chamber, with a minimum pressure drop, leaving the LIBS chamber just below atmospheric pressure. Preliminary measurements revealed an increase of about 50% in analyte signal when using suction to draw the carrier gas flow, rather than positive pressure to force the flow through both chambers.

Laser ablation was achieved using a frequency-tripled Nd:YAG laser (355 nm, 10 ns pulse width) focused on the sample target surface using a 100 mm focal length lens. The ablation laser pulse energy was set to about 25 mJ per pulse for all experiments. The aerosol LIBS plasma was created using a Nd:YAG laser operating at the fundamental frequency (1064 nm, 10 ns pulse width), operating at about 175 mJ per pulse. The laser was focused approximately 6 mm from the exit plane of the transport tube using a 75 mm focal length lens. The resulting plasma emission was collected in backscattering using the same focusing lens, and then split from the incident beam path using a pierced-mirror, and subsequently focused onto a fiber optic bundle and coupled to a 0.275 m spectrometer (2400 groove mm^{-1} grating, 0.15 nm resolution), where emission was recorded using an intensified charge coupled device (ICCD). The detector gate and width were optimized for each analyte atomic emission line. For iron and manganese analysis, a spectral window centered at 250 nm was used for analysis of the 259.37 Mn II line (0–38,543 cm^{-1}) and the 259.94 nm Fe I line (0–38,459 cm^{-1}).

The ablation laser and the analytical LIBS laser pulses were synchronized such that both fired at the same instant. As a consequence, the carrier gas flow rate was then optimized such that the bulk of the ablation plume reached the center of the analytical plasma focal volume at the moment the LIBS laser fired, ensuring a maximum analyte sensitivity. The optimal suction rate was determined to be 0.1 lpm, as measured by the maximum atomic emission line signal-to-noise ratio. We note that an additional local maximum in the SNR was realized for a carrier gas flow rate about twice this value, leading to the conclusion that the optimal condition actually corresponds to analysis of the ablation event from two laser shots previous, rather than the previous shot. This is attributed to less particle loss while transporting the ablation plume at a slower velocity, which most likely minimized overall turbulence.

Using the above parameters, a set of 6 reference materials were analyzed, as summarized in Table 2. The metallic samples were all standard reference materials, while the two glasses were manufactured as follows. Briefly, the glass matrix consists of 52.8% SiO_2, 17.7% CaO and 28.2% K_2O, as determined by reconstitution and XRF. The matrix glass was pulverized and weighed into alumina crucibles together with calculated amounts of MnO, Cr_2O_3, NiO and Fe_2O_3. The powders were mixed thoroughly, then melted at 1400 °C and tilted a few times for better mixing. The matrix glass has its glass transition point at approximately 630 °C, and the melting point at around 920 °C, as measured by DSC.

As observed in Table 2, the samples cover a broad range of material types, including an aluminium alloy, a copper–nickel alloy, an iron–chromium alloy, a high iron steel, and two glasses, with the Mn/Fe ranging by more than two orders of magnitude. Overall, such a disparate set of materials would be expected to yield considerable variations in the laser–material interactions, and in the resulting plasma formation and analyte atomic

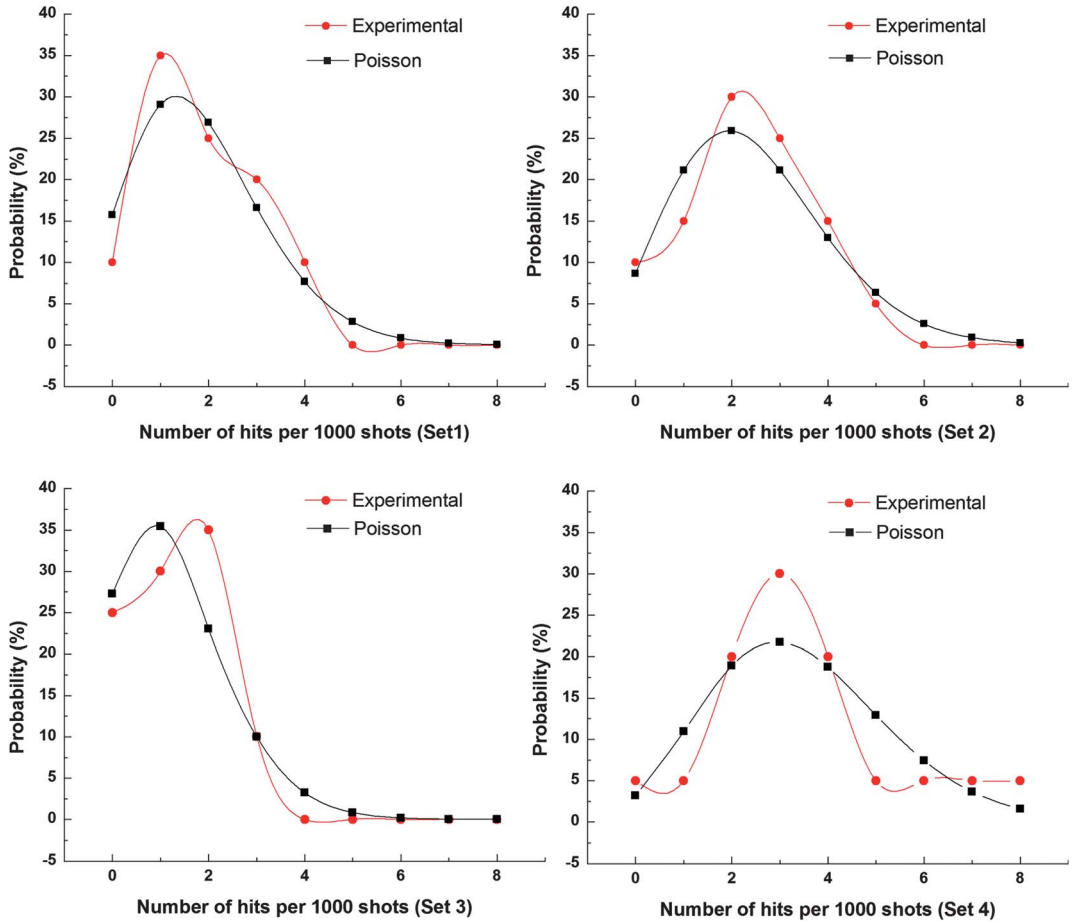

Fig. 2 Sampling probability of aerosol particles in the LIBS plasma volume corresponding to the observed experimental results and to the calculated Poisson distribution for the Table 1 data.

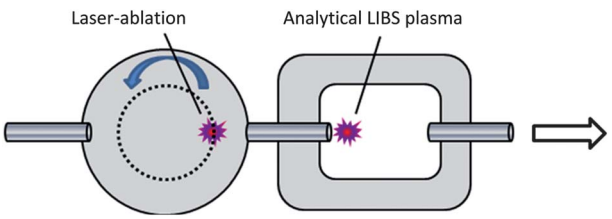

Fig. 3 Schematic of the LA-LIBS sample chamber.

Table 2 Reference materials used for LA-LIBS measurements

Sample	Iron (%)	Manganese (%)
SM-10, Al-alloy	1.96	0.30
1276-a, Cu–Ni alloy	0.56	1.01
1297, Fe–Cr alloy	69.4	7.11
1761, High Fe	95.3	0.68
Glass 1, Si–K–Ca	0.64	1.12
Glass 2, Si–K–Ca	0.27	0.66

emission signals, with the consequence of expected matrix effects with regard to calibration; hence the common need for matrix-matched standards with LIBS. As a whole, this set of samples was selected to challenge the LA-LIBS technique with regard to relative analyte concentrations.

For all LA-LIBS measurements, an average spectrum was recorded prior to any laser ablation; hence representative of the baseline analytical plasma in the nitrogen carrier gas. For each sample, an ensemble-average corresponding to 300 individual laser pulses was recorded, and the procedure was repeated in triplicate. Because the overall LIBS plasma was unchanged with the presence of the ablation particles, which is considered a key indicator of the robustness of the analytical plasma, baseline subtraction was used in which the average baseline spectrum was subtracted from each LA-LIBS spectrum. This process is illustrated in Fig. 4 for a single 300-shot average spectrum corresponding to the NIST 1297 Fe–Cr reference material.

This process was repeated for all samples, and the integrated atomic emission signals (full peak area) were calculated for both the iron and manganese peaks using the baseline-subtracted spectra of each 300-shot dataset. The relative manganese-to-iron ratio (Mn/Fe) was then calculated directly from the ratio of the peak areas, with experimental results plotted against the known reference Mn/Fe mass ratios in Fig. 5. As observed in the figure, the resulting calibration curve of relative Mn/Fe concentrations revealed a linear response ($R = 0.978$) and a near-zero y-intercept, despite the wide disparity in the overall sample matrices. Such a curve demonstrates the potential of the LA-LIBS

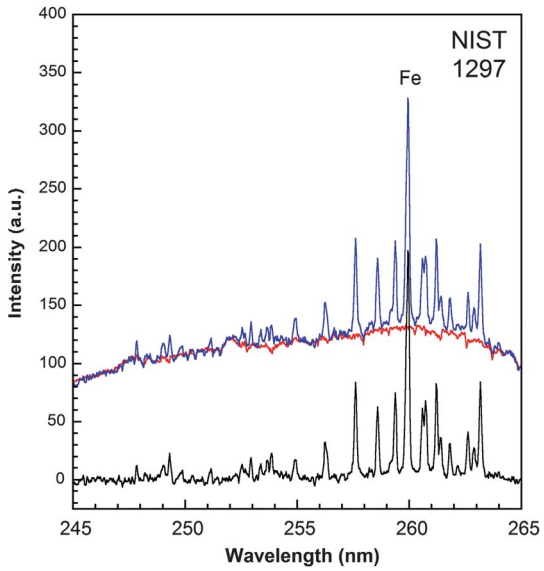

Fig. 4 LA-LIBS spectrum recorded for the NIST 1297 alloy, along with the baseline (*i.e.* no ablation) analytical plasma spectrum (upper two spectra), and the resulting baseline-subtracted spectrum (lower spectrum). The NIST 1297 spectra correspond to a single 300-shot ensemble average.

approach by taking advantage of the ideal characteristics of LIBS for direct analysis of aerosol nanoparticles, thereby largely mitigating the matrix effects realized with direct solids analysis.

In the present study, traditional LIBS for direct analysis of the six bulk solids was not performed. However, in a recent study, the same four metallic species were analyzed using both direct LIBS and the LA-LIBs methodology,[18] and the LA-LIBS approach was found to produce superior analytical performance as measured by both the calibration curve correlation coefficient and the *y*-intercept values. Based on the previous study, inclusion of glass samples along with metallic samples is expected to make worse the analytical calibration curves realized with the direct LIBS analysis. As demonstrated with the current LA-LIBS experiments, the careful design of direct LIBS-based aerosol analysis may be combined with a traditional laser-ablation approach to bulk materials sampling to uncouple matrix-dependent laser-sampling effects from the analytical plasma. Such an approach takes advantages of the applicability of LIBS for rapid and direct analysis of solids, in combination with the analytical plasma independence and robustness, including the use of baseline subtraction. As observed in the present study, relative concentration measurements for a disparate range of material samples, including non-metallic and metallic samples, were realized with the LA-LIBS scheme. Such an approach holds significant promise as a step toward non-matrix matched standards for LIBS analysis.

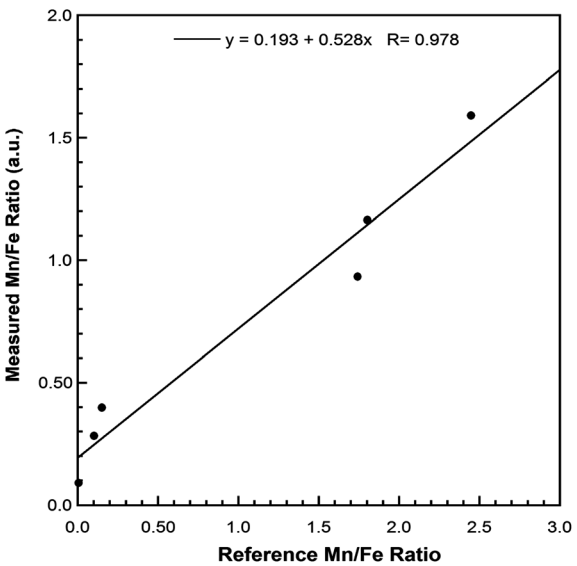

Fig. 5 Calibration curve of the relative Mn/Fe ratio for the LA-LIBS data corresponding to the six sample specimens reported in Table 2.

Alternative approaches to sampling of nanoparticles using LIBS

As discussed above, analysis of fine and ultrafine particles using LIBS can be challenging owing to sampling issues specifically due to the discrete nature of the LIBS plasma resulting in poor sampling statistics and calibration inaccuracies. Sampling issues arise from the point-based sampling nature of LIBS plasma volume which is typically of the order of a few cubic millimetres.[22] Sampling efficiency can be as low as 0.1%, which limits the use of LIBS for real time measurements of ultra-dilute aerosol.[1,23] Additionally, for fine and ultrafine particles, the amount of mass available for detection and analysis in the LIBS plasma is miniscule, which adds to the complexity of the measurement. In order to overcome these challenges, alternative approaches have been developed for nanoparticle analysis using LIBS which typically involve spatial pre-concentration or enrichment of aerosol particles followed by LIBS analysis. Fig. 6(a–d) shows LIBS based approaches pursued by different researchers for aerosol analysis, which can be classified into two main categories: *in situ* measurements [Fig. 6(a) and (b)] and substrate-based measurements [Fig. 6(c) and (d)]. *In situ* measurement of aerosol particles in free streams has been studied and discussed in detail by Hahn and co-workers in numerous studies [Fig. 6(a)].[1–6] They have shown that by using *in situ* analysis, absolute detection limits in the fg range can be obtained.[21] The approach, though, is limited by sampling statistics resulting in poor detection limits in terms of air

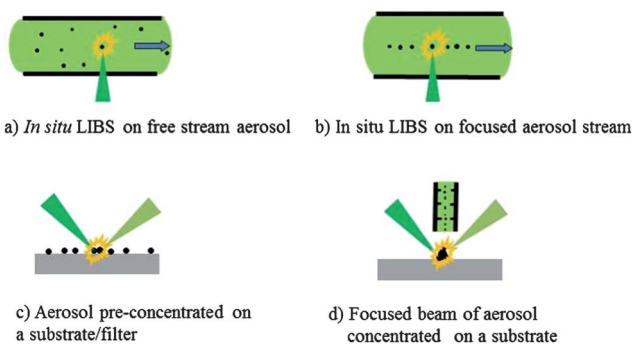

Fig. 6 Common approaches for aerosol analysis using LIBS.

concentration, as demonstrated in the first set of experiments reported here. Detection limits in terms of air concentration obtained by *in situ* analysis ranges from 2–430 μg m^{-3}.[26,27] Cheng developed and implemented an *in situ* approach for LIBS aerosol measurement by concentrating and aligning the aerosol stream into a narrow beam by using a focusing nozzle [Fig. 6(b)].[28] This focusing resulted in increased concentration of aerosol particles in the plasma volume, and thereby resulting in improved sampling efficiency. Overall, the approach helped in improving the sampling statistics, although the use of a focusing nozzle and aerodynamic lens in a LIBS system has its own challenges, as it requires large pumps and pressure drops (50–100 kPa), and can be operated only for very limited flow rates limiting its usage for portable applications.

For substrate based LIBS system, two main approaches for pre-concentration have been demonstrated, namely (1) deposition of a focused stream of aerosol on a substrate, and (2) deposition of a free stream of aerosol onto a substrate or filter. Panne and group used filters for aerosol deposition followed by LIBS analysis [Fig. 6(c)].[29] They successfully demonstrated use of the filter-based LIBS approach for aerosol analysis, and obtained detection limits in the range of 0.02–2.73 μg m^{-3} using 70 mJ per pulse laser energy and a collection time ranging from 1–32 minutes. Park *et al.* used an aerodynamic lens for focusing an aerosol stream to a narrow stream, which was then deposited on a substrate followed by LIBS analysis, resulting in improved sampling statistics as compared to *in situ* LIBS for aerosol [Fig. 6(d)].[30] By employing an aerodynamic lens, aerosol pre-concentration was narrowed to a very small area on the substrate, which was then efficiently ablated by the LIBS plasma. There are advantages as well as challenges offered by both these approaches, and the application dictates the preferential use of one over the other. The approaches discussed above may provide substantial improvement in the figures of merit, but still do not resolve some of the critical issues including calibration accuracy, time resolution, sample collection homogeneity, and field portability, not to mention the loss of the ability for single particle analysis. The aerodynamic lens adds additional complexity to the LIBS system, namely requirement of large vacuum pumps and low flow rates making it less suitable for field operations, while filter-based deposition requires aerosol collection over a large surface area resulting in low temporal resolution for aerosol analysis, and calibration inaccuracies due to non-homogenous deposition of aerosol sample on the substrate.

In a recent study, Diwakar *et al.* developed a novel approach for near real-time analysis of aerosols using LIBS by employing pre-concentration of the aerosol using an electrostatic deposition method.[13] The approach involves electrostatically charging the nanoparticles using a corona field generated between two microneedles by applying high voltage across the needles (Fig. 7), followed by deposition of the particles on the exposed tip of one of the microneedles (500 μm diameter). The collection unit was designed such that only the surface of the needle tip is exposed, while the walls of the needle were insulated. After the particles were deposited on the electrode for a few seconds to a few minutes, the LIBS analysis was performed using a low energy pulsed laser (Nd:YAG, 20 mJ per pulse). By changing the collection time, mass loading on the micro-needle tip was varied. Mass loading on the needle tip was determined by counting the number of particles before and after the charging and collection of aerosols using a condensation particle counter (CPC).

Fig. 8 (inset) shows the LIBS signal from the 510.55 nm Cu emission line (11,203–30,784 cm^{-1}) for a copper-laden aerosol stream which was deposited for 1, 2 and 3 minutes respectively. Fig. 8 also shows typical calibration curve obtained in the experiment, which is fairly linear over a wide range of mass loadings. Various elements were studied using this system, and the mass detection limits in the range of 0.018–5 ng were obtained for Cd, Cr, Cu, Mn, Na, and Ti.[13] The RSD of the measurements varied in the range of 1–21% for lower mass loadings, while it was below 10% for higher mass loadings, which shows a significant improvement as compared to *in situ* LIBS measurements, with

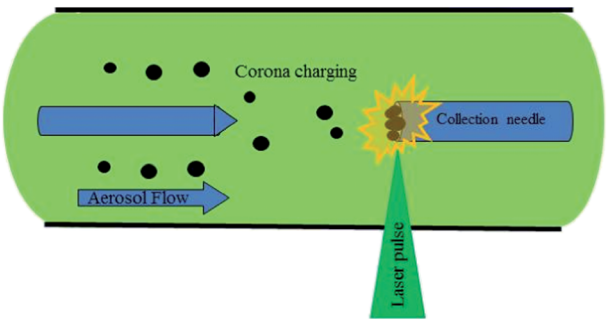

Fig. 7 Novel approach for aerosol nanoparticle analysis using electrostatic charging and collection on a microneedle.

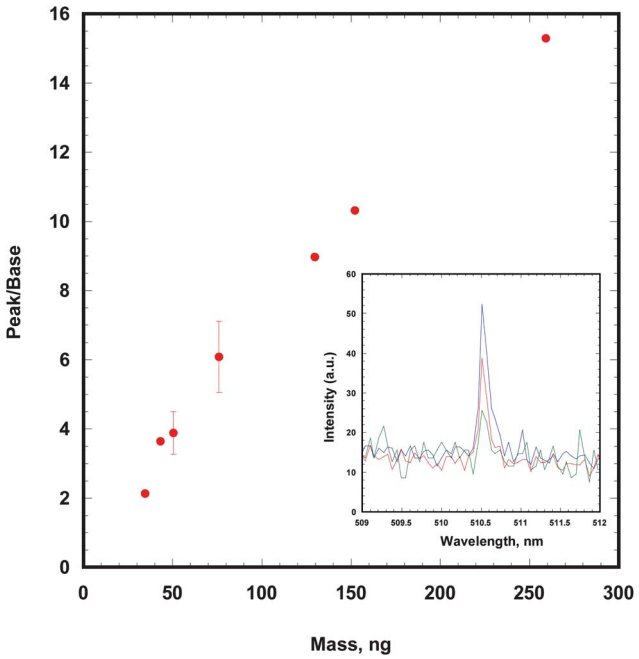

Fig. 8 Typical calibration curve obtained using electrostatic charging and collection based LIBS system.[13] Cu calibration curve is shown here as a representative calibration curve (510.55 nm emission line). Monodisperse aerosol particles of 80 nm were nebulized and deposited on microelectrode using electrostatic collection as described by Diwakar *et al.*[13] Inset shows typical LIBS signal for Cu for different mass loading of 1,2, and 3 minutes respectively. Representative error bars shown are ± one standard deviation.

RSDs typically in the 25–42%.[27,28,31] The electrostatic pre-concentration technique developed by Diwakar *et al.* has many advantages over other substrate-based methods involving aerosol nanoparticle collection on a filter or focused deposition using an aerodynamic lens. Because the particle mass is collected over a very small area that is smaller or comparable to the spatial extent of the laser-induced plasma, the entire mass is available for analysis. Electrostatic charging and pre-concentration of aerosol provides a well-controlled approach of delivering a known amount of analyte mass on the micro-electrode, while considerably improving reliability of the calibration and enhancing the measurement accuracy and precision. Further, the aerosol collection technique can be operated at high flow rates and does not require bulky pumps for operation, making it well suited for field portable instrumentation. Nice temporal resolution (from a few seconds to few minutes) is another major advantage offered by this approach.

Discussion and conclusions

Clearly the use of the LIBS technique for analysis of micro- and nanoparticle systems provides many opportunities, from analysis of ablation particles, to process monitoring, to environmental monitoring. The successful application of LIBS for particle analysis is advanced by a thorough understanding of the relevant physical processes, allowing one to optimize the analytical signal with regard not only to signal-to-noise ratio, but with regard to minimization of matrix effects by allowing sufficient plasma resident time for the necessary heat and mass transfer processes to occur. The related aerosol particle sampling rate requires an examination of the LIBS-based aerosol analysis problem in the context of discrete aerosol particles, and a finite (*i.e.* discrete) plasma sampling volume. Such an understanding is useful for elucidating key regimes suited to ensemble-averaging and those suited to more sophisticated data analysis approaches due to aerosol sampling limitations. As demonstrated in this study, aerosol particle analysis with LIBS is nicely modeled by the Poisson distribution, allowing one to model alternative analysis methods and strategies, such as a conditional analysis algorithm to enhance the signal-to-noise ratio.

As demonstrated with the current LA-LIBS experiments, the careful design of direct LIBS-based aerosol analysis may be combined with a traditional laser-ablation approach to bulk materials sampling to uncouple matrix-dependent laser-sampling effects from the analytical plasma. Such an approach takes advantages of the high applicability of LIBS for direct analysis of nanoparticles in aerosol form, including the use of baseline subtraction. As observed in the present study, relative concentration measurements for a disparate range of material samples, including non-metallic and metallic samples, were realized with the LA-LIBS scheme. Such an approach holds significant promise as a step toward non-matrix matched standards for LIBS analysis.

Finally, LIBS offers immense potential for near real-time multi-elemental analysis of aerosol systems, as has been demonstrated by numerous studies over the years. Still, there are several challenges for analysis of fine and ultrafine aerosol particles using *in situ* LIBS approach mainly due to discrete nature of the LIBS plasma in combination with low sampling rates. Several pre-concentration approaches have been developed for improving the sampling of aerosols in LIBS, namely substrate/filter based systems and aerosol focusing based systems. These approaches improve sampling of aerosol systems, but also add certain limitations and complexities to the LIBS system which sometimes work against the recognized strengths of LIBS as an analytical tool, namely its simplicity and robustness. We examined data using a novel approach combining an electrostatic charging and collection method for pre-concentration of aerosol nanoparticles on a microneedle followed by LIBS analysis. The approach offers numerous advantages in terms of simplicity, robustness, field portability, calibration accuracy, temporal resolution and low detection limits, and shows promise for qualitative and quantitative nanoanalysis.

In summary, the future of LIBS for micro- and nanoparticle analysis holds great promise, offering many experimental options which should be considered in combination with the specific applications. Clearly the use of LIBS for nanoparticle analysis has benefitted from careful assessment of the key physical processes, which has helped to guide innovative approaches.

Acknowledgements

The work was funded in part by the National Science Foundation through grant CHE-0822469, as part of the Plasma–Analyte Interaction Working Group, a collaborative effort of the University of Florida, Federal Institute of Materials Research and Testing (BAM) in Berlin, and the Institute for Analytical Sciences (ISAS) in Dortmund, jointly funded by the NSF and DFG. The microneedle aerosol sampling study was conducted at NIOSH, Cincinnati. PKD would like to thank Pramod Kulkarni (NIOSH) for his help, support and guidance.

References

1 D. W. Hahn, W. L. Flower and K. R. Hencken, Discrete particle detection and metal emissions monitoring using laser-induced breakdown spectroscopy, *Appl. Spectrosc.*, 1997, **51**, 1836–1844.
2 D. W. Hahn and M. M. Lunden, Detection and analysis of aerosol particles by laser-induced breakdown spectroscopy, *Aerosol Sci. Technol.*, 2000, **33**, 30–48.
3 J. E. Carranza and D. W. Hahn, Sampling statistics and considerations for single-shot analysis using laser induced breakdown spectroscopy, *Spectrochim. Acta, Part B*, 2002, **57**, 779–790.
4 V. Hohreiter and D. W. Hahn, Plasma–particle interactions in a laser-induced plasma: implications for laser-induced breakdown spectroscopy, *Anal. Chem.*, 2006, **78**, 1509–1514.
5 D. W. Hahn, Laser-induced breakdown spectroscopy for analysis of aerosol particles: the path toward quantitative analysis, *Spectroscopy*, 2009, **24**, 26–33.
6 P. K. Diwakar, P. B. Jackson and D. W. Hahn, Investigation of multi-component aerosol particles and the effect on quantitative laser-induced breakdown spectroscopy: consideration of localized matrix effects, *Spectrochim. Acta, Part B*, 2007, **62**, 1466–1474.
7 P. K. Diwakar, S. Groh, K. Niemax and D. W. Hahn, Study of analyte dissociation and diffusion in laser-induced plasmas: implications for laser-induced breakdown spectroscopy, *J. Appl. Spectrosc.*, 2010, **25**, 1921–1930.
8 R. E. Neuhauser, U. Panne, R. Niessner, G. A. Petrucci, P. Cavalli and N. Omenetto, On-line and *in situ* detection of lead aerosols by plasma-spectroscopy and laser-excited atomic fluorescence spectroscopy, *Anal. Chim. Acta*, 1997, **346**, 37–48.
9 J. E. Carranza, B. T. Fisher, G. D. Yoder and D. W. Hahn, On-line analysis of ambient air particles using laser-induced breakdown spectroscopy, *Spectrochim. Acta, Part B*, 2001, **56**, 851–864.

10 T. Amodeo, C. Dutouquet, F. Tenegal, B. Guizard, H. Maskrot, O. Le Bihan and E. Frejafon, On-line monitoring of composite nanoparticles synthesized in a pre-industrial laser pyrolysis reactor using laser-induced breakdown spectroscopy, *Spectrochim. Acta, Part B*, 2008, **63**, 1183–1190.

11 N. Strauss, C. Fricke-Begemann and R. Noll, Size-resolved analysis of fine and ultrafine particulate matter by laser-induced breakdown spectroscopy, *J. Anal. At. Spectrom.*, 2010, **25**, 867–874.

12 G. Gallou, J. B. Sirven, C. Dutouquet, L. Le Bihan and E. Frejafon, Aerosols analysis by LIBS for monitoring of air pollution by industrial sources, *Aerosol Sci. Technol.*, 2011, **45**, 918–926.

13 P. Diwakar, P. Kulkarni and M. E. Birch, New approach for near-real-time measurement of elemental composition of aerosol using laser-induced breakdown spectroscopy, *Aerosol Sci. Technol.*, 2012, **46**, 316–332.

14 B. R'mili, C. Dutouquet, J. B. Sirven, O. Aguerre-Chariol and E. Frejafon, Analysis of particle release using LIBS and TEM samplers when handling CNT (carbon nanotube powders), *J. Nanopart. Res.*, 2011, **13**, 563–577.

15 C. Janzen, R. Fleige, R. Noll, H. Schwenke, W. Lahmann, J. Knoth, P. Beaven, E. Jantzen, A. Oest and P. Koke, Analysis of small droplets with a new detector for liquid chromatography based on laser-induced breakdown spectroscopy, *Spectrochim. Acta, Part B*, 2005, **60**, 993–1001.

16 S. Groh, P. K. Diwakar, C. C. Garcia, A. Murtazin, D. W. Hahn and K. Niemax, 100% efficient sub-nanoliter sample introduction in laser-induced breakdown spectroscopy and inductively-coupled plasma spectrometry: implications for ultralow sample volumes, *Anal. Chem.*, 2010, **82**, 2568–2573.

17 F. J. Fortes, L. M. Cabalin and J. J. Laserna, Laser-induced breakdown spectroscopy of solid aerosols produced by optical catapulting, *Spectrochim. Acta, Part B*, 2009, **64**, 642–648.

18 B. C. Windom and D. W. Hahn, Laser-ablation-laser induced breakdown spectroscopy (LA-LIBS):a means for overcoming matrix effects leading to improved analyte response, *J. Anal. At. Spectrom.*, 2009, **24**, 1665–1675.

19 A. P. M. Michel, Review: applications of single-shot laser-induced breakdown spectroscopy, *Spectrochim. Acta, Part B*, 2010, **65**, 185–191.

20 V. Zorba, X. L. Mao and R. E. Russo, Ultrafast laser-induced breakdown spectroscopy for high spatial resolution chemical analysis, *Spectrochim. Acta, Part B*, 2011, **66**, 189–192.

21 P. B. Dixon and D. W. Hahn, On the feasibility of detection and identification of individual bioaerosols using laser-induced breakdown spectroscopy, *Anal. Chem.*, 2005, **77**, 631–638.

22 J. E. Carranza and D. W. Hahn, Plasma volume considerations for analysis of gaseous and aerosol samples using laser induced breakdown spectroscopy, *J. Anal. At. Spectrom.*, 2002, **17**, 1534–1539.

23 B. Hettinger, V. Hohreiter, M. Swingle and D. W. Hahn, Laser-induced breakdown spectroscopy for ambient air particulate monitoring: correlation of total and speciated aerosol counts, *Appl. Spectrosc.*, 2006, **60**, 237–245.

24 G. McPherson, *Statistics in Scientific Investigation*, Springer-Verlag, New York, 1990.

25 J. E. Carranza, K. Iida and D. W. Hahn, Conditional data processing for single-shot spectral analysis by use of laser-induced breakdown spectroscopy, *Appl. Opt.*, 2003, **42**, 6022–6028.

26 B. T. Fisher, H. A. Johnsen, S. G. Buckley and D. W. Hahn, Temporal gating for the optimization of laser-induced breakdown spectroscopy detection and analysis of toxic metals, *Appl. Spectrosc.*, 2001, **55**, 1312–1319.

27 T. Amodeo, C. Dutouquet, O. Le Bihan, M. Attoui and E. Frejafon, On-line determination of nanometric and sub-micrometric particle physicochemical characteristics using spectral imaging-aided laser-induced breakdown spectroscopy coupled with a scanning mobility particle sizer, *Spectrochim. Acta, Part B*, 2009, **64**, 1141–1152.

28 M. D. Cheng, Field measurement comparison of aerosol metals using aerosol beam focused laser-induced plasma spectrometer and reference methods, *Talanta*, 2003, **61**, 127–137.

29 U. Panne, R. E. Neuhauser, M. Theisen, H. Fink and R. Niessner, Analysis of heavy metal aerosols on filters by laser-induced plasma spectroscopy, *Spectrochim. Acta, Part B*, 2001, **56**, 839–850.

30 K. Park, G. Cho and J. H. Kwak, Development of an aerosol focusing-laser induced breakdown spectroscopy (aerosol focusing-LIBS) for determination of fine and ultrafine metal aerosols, *Aerosol Sci. Technol.*, 2009, **43**, 375–386.

31 G. A. Lithgow, A. L. Robinson and S. G. Buckley, Ambient measurements of metal-containing PM2.5 in an urban environment using laser-induced breakdown spectroscopy, *Atmos. Environ.*, 2004, **38**, 3319–3328.